Protein Engineering, Design & Selection vol. 21 no. 5 pp. 319–327, 2008
doi:10.1093/protein/gzn009

Directed evolution on the cold adapted properties of TAB5 alkaline phosphatase

Dimitris Koutsioulis[1], Ellen Wang[2], Maria Tzanodaskalaki[3], Dimitra Nikiforaki[1], Alexandra Deli[1], Georges Feller[4], Pirkko Heikinheimo[2,5] and Vassilis Bouriotis[1,3,6]

[1]Department of Biology, Enzyme Biotechnology Group, University of Crete, PO Box 2208, Vasilika Vouton, 71409 Heraklion, Crete, Greece, [2]NORSTRUCT, Institute of Chemistry, University of Tromsø, N-9037 Tromsø, Norway, [3]Institute of Molecular Biology and Biotechnology, PO Box 1527, Vasilika Vouton 71110, Heraklion, Crete, Greece, [4]Laboratory of Biochemistry, University of Liège, Institute of Chemistry B6a, B-4000 Liège-Sart Tilman, Belgium and [5]Institute of Biotechnology, University of Helsinki, PO Box 65, FIN-00014 Helsinki, Finland

[6]To whom correspondence should be addressed. E-mail: bouriotis@imbb.forth.gr (V.B.); dkoutsioulis@hotmail.com or dkoutsioulis@gmail.com (D.K.)

Psychrophilic alkaline phosphatase (AP) from the Antarctic strain TAB5 was subjected to directed evolution in order to identify the key residues steering the enzyme's cold-adapted activity and stability. A round of random mutagenesis and further recombination yielded three thermostable and six thermolabile variants of the TAB5 AP. All of the isolated variants were characterised by their residual activity after heat treatment, Michaelis–Menten kinetics, activation energy and microcalorimetric parameters of unfolding. In addition, they were modelled into the structure of the TAB5 AP. Mutations which affected the cold-adapted properties of the enzyme were all located close to the active site. The destabilised variants H135E and H135E/G149D had 2- and 3-fold higher k_{cat}, respectively, than the wild-type enzyme. Wild-type AP has a complex heat-induced unfolding pattern while the mutated enzymes loose local unfolding transitions and have large shifts of the T_m values. Comparison of the wild-type and mutated TAB5 APs demonstrates that there is a delicate balance between the enzyme activity and stability and that it is possible to improve the activity and thermostability simultaneously as demonstrated in the case of the H135E/G149D variant compared to H135E.

Keywords: catalysis/directed evolution/mutagenesis/psychrophilic enzymes/thermostability

Introduction

Psychrophilic organisms are widely distributed in nature as a large part of the Earth's surface is at temperatures around 0°C. These cold-loving microorganisms face the thermodynamic challenge to maintain enzyme-catalysed reactions and metabolic rates compatible with sustained growth near or below the freezing point of pure water (D'Amico *et al*., 2002; Margesin *et al*., 2002). Typically, the rate of a biochemical reaction decreases 2–3-fold when the temperature is lowered by 10°C. Consequently, the activity of an enzyme will be 16–80 times lower at 0°C than that at 37°C. In order to withstand this, enzymes from psychrophilic organisms have high catalytic activity at low temperatures and low thermal stability (Smalas *et al*., 2000; Feller, 2003). Due to these properties, cold-adapted enzymes have high potential in basic research as well as for applications in the detergent and food industries (Gerday *et al*., 2000; Cavicchioli *et al*., 2002).

Comparison of the structures and sequences of enzymes adapted to different temperatures has provided important insights into the structural basis of protein adaptation (Fields and Somero, 1998; Zavodszky *et al*., 1998; Gianese *et al*., 2002) but not general rules. Natural homologs adapted to different temperatures are often separated by large evolutionary distances which complicate such analysis. Ignorance of the natural selection pressure makes it difficult to identify mutations which reflect temperature adaptation from those which merely respond to other environmental conditions (Miyazaki *et al*., 2000; Wintrode and Arnold, 2000). In addition, protein stability is a result of a complex interplay of forces and a delicate balance between stabilising and destabilising interactions (Jaenicke *et al*., 1996; Richards, 1997).

Protein engineering is a wonderful tool to study specific adaptive mechanisms in a more controlled way (Yano and Poulos, 2003). Rational, knowledge-based and non-rational, random mutagenesis are the two parallel approaches of protein design (Arnold, 2001). Rational protein design has identified several specific mechanisms for temperature adaptation (D'Amico *et al*., 2001; Mavromatis *et al*., 2003), but engineering highly stable and active enzymes is still a difficult challenge by this approach. Random mutagenesis opens more possibilities which are difficult to find through rational approaches, due to our incomplete structural and functional knowledge on protein cold adaptation.

Directed evolution is an efficient tool for improving a wide variety of enzyme properties even without structure–function information (Dalby, 2003). The process mimics natural Darwinian evolution, and yields diverse pools of mutation libraries which are generated by *in vitro* random mutagenesis and gene recombination. In several cases, this has led to amino acid changes that would not have been suggested by rational approaches (Spiller *et al*., 1999; Martin *et al*., 2001; Wintrode *et al*., 2001).

Alkaline phosphatases (APs, EC 3.1.3.1) are homodimeric metalloenzymes that catalyse the hydrolysis and transphosphorylation of a wide variety of phosphate monoesters (Coleman and Gettins, 1983). We have previously reported the cloning, sequencing and overexpression of the gene encoding AP from the Antarctic strain TAB5 (Rina *et al*., 2000). This protein displays the typical properties of cold-adapted enzymes: high catalytic activity at low temperatures and relative instability at high temperatures. Earlier site-directed mutagenesis and enzyme characterisation suggested that local flexibility and glycine clusters are important for the psychrophilic character and catalytic properties of TAB5 AP (Tsigos *et al*., 2001; Mavromatis *et al*., 2002).

We have subjected the cold-adapted TAB5 AP into laboratory evolution pressure in order to identify specific residues important for enzyme activity and stability. Selected variants of this enzyme which had different temperature adaptations than the wild type were characterised by the calculation of activation parameters. In addition, the stabilising or destabilising effects of the mutations were studied by modelling the changes into the crystal structure of the TAB5 AP (Wang *et al*., 2007) (pdb, 2iuc). Finally, the intricate relationship of activity and stability in the psychrophilic AP was examined by comparing the thermal stabilities and temperature-dependent activities of mutated enzymes.

Materials and methods

Construction of pRSETWT

TAB5 AP gene was cloned in a construction called pN1 (Rina *et al*., 2000). We further removed the first 22 amino acids from the N-terminus by PCR using the upstream primer PhoNFor (5'-CAA AAC ACA TAT GGT TTT AGT AAA AAA TGA GC-3', *Nde*I restriction site underlined) and the downstream primer PhoRev (5'-TTG AAT TCG TTT ATT GAT TCC ACT TTG-3', *Eco*RI restriction site underlined) using pN1 as template.

The PCR reaction mixtures were incubated in an Eppendorf thermal cycler (Mastercycler gradient) for 30 cycles of 94°C for 1 min, 47°C for 1 min and 72°C for 1 min. The amplified product was isolated by agarose gel electrophoresis, gel purified using QIAEX (Qiagen) and digested with *Nde*I and *Eco*RI. The resulting *Nde*I/*Eco*RI fragment was inserted into the pRSETA vector previously digested with these enzymes. The ligation mixture was used to transform competent cells of *Escherichia coli* strain DH5 alpha resulting in plasmid pRSETWT.

Random mutagenesis

The first generation mutation library was created by error-prone PCR (Cadwell and Joyce, 1994). The AP gene was amplified using 40 pmol of PhoNFor and PhoRev and 20 ng of pRSETWT in a 100 μl PCR reaction containing 50 mM KCl, 10 mM Tris–HCl pH 8.5, 0.1% Triton X-100, 7 mM $MgCl_2$, 1 mM dCTP, 1 mM dTTP, 0.2 mM dATP, 0.2 mM dGTP and 9 U *Taq* polymerase (MINOTECH). The reaction was thermocycled for 30 rounds of 94°C for 10 s, 42°C for 30 s and 72°C for 1 min and amplification of the product was confirmed on an agarose gel.

DNA recombination

In vitro recombination of selected variants was done using the staggered extension process (StEP) (Zhao *et al*., 1998). The 50 μl reaction mixture contained 1 x *Taq* reaction buffer, 0.2 mM of each dNTP, 25 pmol of PhoNFor and PhoRev, 0.37 pmol of each plasmid and 1 unit of *Taq* polymerase (MINOTECH). The PCR schedule consisted of 5 min at 94°C followed by 100 cycles of 94°C for 30 s and 50°C for 10 s.

Mutant library construction

Mutagenic PCR or DNA recombination reaction products were inserted into pRSETA vectors as described for pRSETWT and transformed into *E.coli* BL21(DE3) cells, which were plated on Luria-Bertani (LB) agar plates containing 150 μg/ml ampicillin. After 16 h of growth at 30°C, colonies were picked with sterile toothpicks into 200 μl of LB/ampicillin medium on 96-well plates (COSTAR 96 Well Flat Bottom). The cultures were allowed to grow at 30°C for 16 h after which they were duplicated by transferring 60 μl from each well into a new plate. The original plates were stored and the duplicates were used for the screening assay.

Thermostability screening assay

We have developed the following 96-well plate screening assay in order to identify the thermostable or thermolabile AP variants. From each well of the duplicated 96-well plate, 10 μl of cell culture was transferred to the corresponding wells of two new plates. One of these plates was assayed directly for enzyme activity by the addition of 20 μl of 5 mM *p*-nitrophenyl phosphate (*p*NPP) (Sigma) and 100 μl of 1 M diethanolamine-Cl at pH 10, 10% glycerol, 10 mM $MgCl_2$ and 1 mM $ZnCl_2$. Mutants which were less than 20% of parent activity at 15°C were removed and were not further examined. The second plate was heat-treated in an Eppendorf thermal cycler for 45 min at 50°C, chilled on ice for 15 min and assayed for remaining (residual) activity. The AP reaction was monitored in a 96-well plate reader (FLUOSTAR GALAXY, BMG Laboratories) at 405 nm at 15°C. Variants, which had more than 10% enhanced or reduced activity compared to the wild type, were selected for further characterisation.

Site-directed mutagenesis

The double mutant S86A/G87A was constructed by PCR using a two step-four primer overlap/extension method (Horton *et al*., 1990). In order to regenerate the mutation G87A, we used the following primers: forward primer 5'-GAT TCA GCC GCT GCC GCT ACT GCT TTT TCC TGT-3' and reverse primer 5'-AAA AGC AGT AGC GGC AGC GGC TGA ATC AGT TAC-3', the mutated site is underlined. The plasmid pRSETS86A was used as template and the rest of the PCR reaction was performed as described for pRSETWT using upstream primer PhoNFor and downstream primer PhoRev. The resulting plasmid was named as pRSETS86A/G87A.

Overexpression and purification of enzymes

Enzymes were produced as previously described (Tsigos *et al*., 2001) with the following modifications. Protein was produced in *E.coli* BL21(DE3)-pLysS strain. The transformed cells were grown overnight at 30°C in 20 ml LB containing 150 μg/ml ampicillin and 34 μg/ml chloramphenicol. This culture was used to inoculate 1000 ml of fresh medium and antibiotics supplemented with 10 mM $MgSO_4$, 0.4 mM $ZnSO_4$ and 10 mM KCl. Cultures were then transferred to 25°C and at A_{600} of 0.6–0.7, induced with 0.1 mM isopropyl thio-β-D-galactopyranoside. Induced cells were allowed to grow 12–14 h at 20°C. Cells were harvested by centrifugation and frozen at −20°C.

All purification steps were carried out at 8°C if not mentioned. One gram of frozen cells was thawed in a 3 ml of 50 mM Tris–Cl pH 7.6, 200 mM NaCl, 1 mM dithiothreitol (DTT), 0.3 mg/ml lysozyme, 10 μg/ml Dnase I and 10 mM $MgCl_2$. Every 30 min, phenylmethylsulfonyl fluoride was added at 1 mM. After incubation on ice for 2.5 h, they were

centrifuged at 4°C for 20 min at 10 000 g to remove intact cells and cell debris.

The supernatant was collected and diluted 3-fold with 20 mM Tris–Cl pH 7.6, 10 mM $MgCl_2$ (buffer A) and applied onto a Q-Sepharose fast flow column (GE Healthcare). The column was washed with buffer A until A_{280} reached background levels and then eluted with a linear 0–0.1 M KPO_4 (at pH 6) gradient in buffer A over 10 column volumes and subsequently with a linear 0–0.6 M gradient of NaCl in buffer A over 20 column volumes. AP eluted at ~0.1–0.18 M NaCl and activity containing fractions were pooled and concentrated with a Centricon Concentrator 10 (Amicon) to <3 ml. The concentrated sample was loaded onto a Sephacryl S200 high-resolution gel-filtration column (GE Healthcare) (380 ml) with 20 mM Tris–Cl pH 7.6, 10 mM $MgCl_2$ and 200 mM NaCl (buffer B). The column was washed with buffer B and fractions with AP activity were pooled and concentrated as above. Enzyme purity was judged by homogeneous SDS–PAGE (Laemmli, 1970). Protein concentration was determined using Bradford's dye binding assay (Bio-Rad, Bradford, 1976) with bovine serum albumin as the protein standard. Purified enzymes were stored at −20°C with 50% glycerol and 1 mM DTT.

Enzymatic assay

Specific activity was determined in 1 M diethanolamine-Cl pH 10, 10% glycerol, 10 mM $MgCl_2$, 1 mM $ZnCl_2$ and 5 mM *p*NPP at 15°C. The amount of released product, *p*-nitrophenolate, was measured by absorbance at 405 nm on a 96-well plate reader.

Steady-state enzyme kinetics

Steady-state enzyme kinetics was performed in the temperature range 10–30°C. The program HYPER v 1.01 was used to determine V_{max} and K_m values. The k_{cat} values were calculated from V_{max} using a molecular mass of 35 861 Da for TAB5 AP. Reported values are the average of three measurements. The standard deviations do not exceed 5%.

Activation parameters

Thermodynamic parameters of activation were calculated as described (Lonhienne *et al*., 2000) using Eqs. (1–3),

$$\Delta G^{\#} = \mathrm{RT}(\ln(k_B T/h) - \ln k) \quad (1)$$

$$\Delta H^{\#} = E_\alpha - \mathrm{RT} \quad (2)$$

$$\Delta S^{\#} = \frac{\Delta H^{\#} - \Delta G^{\#}}{T} \quad (3)$$

where k_B is the Bolzmann constant, h the Planck constant, E_α the activation energy of the reaction and R the gas constant.

Thermal inactivation of enzymes

For thermal inactivation measurements, enzymes were incubated at 55°C (for 120 min, samples were collected every 5 min) and 60°C (for 60 min, samples were collected every 5 min), in 20 mM Tris–Cl pH 7.6, 10 mM $MgCl_2$, 200 mM NaCl and treatment stopped on ice for 30 min. The remaining activity was measured at 15°C. Reported values are the average of at least two measurements. The standard deviations do not exceed 5%.

Molecular modelling

The structural effects of the mutations were analysed in the crystal structure of TAB5 AP (Wang *et al*., 2007) (pdb, 2iuc). Mutations were made in Coot (Emsley and Cowtan, 2004), with the best approximation to the native residue conformation in TAB5 AP or comparing to the corresponding residue in *E.coli* AP (pdb, 1ed9). Figures were prepared with PyMOL (http://pymol.sourceforge.net) and edited in Photoshop and Corel Draw.

Differential scanning calorimetry (DSC)

Measurements were done using a MicroCal MCS-Differential scanning calorimetry (DSC) instrument at a scan rate of 90 K h^{-1} using 2 atm nitrogen pressure. Samples were dialysed overnight against 30 mM 3-(N-Morpholino) propanesulfonic acid pH 7.5 and the same buffer was used in the reference cell and for buffer baseline determination. Protein concentration was determined by the bicinchoninic acid protein assay (Pierce) and adjusted to ~4 mg/ml. Calorimetric enthalpies (ΔH_{cal}) were determined as the area of the transitions, normalised for protein concentration, limited by a linear baseline drawn between the start (fixed at 30°C) and the visible end of the transitions. In the case of wild-type AP and the stabilised mutants, datapoints above 70°C were excluded due to the exothermic signal drift of aggregation.

Results

Directed evolution of TAB5 AP

A key element of any directed evolution experiment is a rapid and sensitive screen, which can record even small changes in thermostability due to the single amino acid substitutions (Zhao and Arnold, 1997; Lin and Cornish, 2002). In this study, we have developed a screen which is based on the retention of activity of the mutant enzymes following incubation at an elevated temperature (Giver *et al*., 1998). Variants with comparable initial activity to the wild type but altered activity after heat treatment were selected for further analysis.

The first generation mutation library was created by error prone PCR (Cadwell and Joyce, 1994) of wild-type AP on pRSETWT under conditions adjusted to generate an average of one to two amino acid substitutions per gene which is considered optimal for the improvement of specific properties of the wild-type AP (Arnold and Moore, 1997). We screened approximately 13 000 clones for activity and thermostability. From this pool, we isolated three thermostable and three thermolabile clones based on their activities before and after incubation at 50°C. Each variant had only one amino acid substitution.

We then recombined *in vitro* the advantageous mutations from the first generation on three separate recombination libraries using the StEP method (Zhao *et al*., 1998). The first library contained the thermostable mutations at amino acids 86, 87 and 149 and the second recombined genes with thermolabile variants at amino acids 42, 135 and 338. The third library recombined all six sites. A total of 1000 clones in each library were assayed before and after incubation at 50°C. The screening of the first library did not reveal new mutations or combinations of the parental mutations which

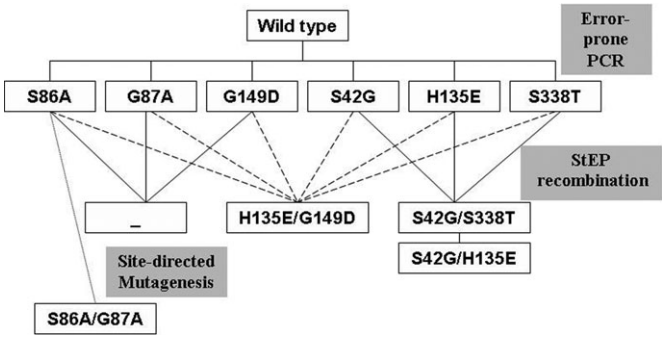

Fig. 1. Lineage of psychrophilic alkaline phosphatase variants. First generation variants were created by error-prone PCR. The six mutations selected from the first generation variants were recombined by StEP in three different combinations. Site-directed mutagenesis was used to create double mutant S86A/G87A. Only non-synonymous mutations are shown.

would have had significant changes in their cold-adapted functional properties (Fig. 1). Three thermolabile double variants were selected from the other two libraries: S42G/H135E, S42G/S338T and H135E/G149D. The overall strategy and the selected variants are summarised in Fig. 1.

Site-directed mutagenesis

It was quite unlikely that we would obtain a double mutant containing both mutations S86A and G87A by StEP or any other *in vitro* DNA recombination technique, due to the close proximity of these sites. However, we wanted to study if the thermostability effects on these two mutations were additive, thus we designed the double mutant by using standard PCR methods (Horton *et al*., 1990).

Thermal inactivation of mutant and wild-type enzymes

In order to investigate the effects of mutations on the maintenance of activity of the psychrophilic AP after thermal treatment, purified enzymes were incubated at 55 and 60°C and subsequently their remaining activity was measured. Mutations S86A, G87A and G149D stabilise the TAB5 AP (Table I). The combination of the mutations in positions 86 and 87 resulted in further stabilisation. After 2 h incubation at 60°C, the variant S86A/G87A retained 33% of its activity, which is about 66 times more than the wild-type enzyme does (Table I).

Mutations S42G, H135E and S338T resulted in enzymes with decreased residual activity. After 5 min at 60°C, H135E and the double mutant S42G/S338T retained only 0.6 and 0.9% of their activities, about 10 and 7 times lower that of the wild-type TAB5 AP (Table I).

Temperature dependence of activity in wild-type and mutant enzymes

We have measured the enzyme kinetics of all mutants over the entire range of temperature (10–30°C) where the wild-type TAB5 AP is stable (Fig. 2). Mutants H135E and H135E/G149D are the most active. The catalytic turnover (k_{cat}) at 30°C for these variants was 2- and 3-fold higher than the k_{cat} of the wild-type (Fig. 2A). However, the K_m values of these variants were greatly increased compared to the wild-type TAB5 AP values (Fig. 2C). The rest of the variants have reduced k_{cat} values compared to the wild-type enzyme (Fig. 2B). The variant S86A/G87A has the lowest activity, which at 30°C is seven times lower than the wild-type activity (Fig. 2B).

Table I. Thermal inactivation of wild-type and mutant APs at 55°C and 60°C

	Initial activity (%)	Remaining activity (%)			
Incubation time (min)	0	5	120	5	60
Temperature (°C)		55	60		
WT	100	15	2.4	6	0.5
S86A	100	69.2	15.6	25	9
G87A	100	49.5	11.4	17.1	7.1
G149D	100	29.6	2.8	13.2	0.7
S86A/G87A	100	54	39.4	57.5	33
H135E/G149D	100	24.5	1	1.3	0.4
S42G	100	14.5	0	3.7	0
H135E	100	5.8	0.4	0.6	0
S338T	100	17.7	0.6	4.8	0
S42G/H135E	100	13.3	0	3.8	0
S42G/S338T	100	6.7	0	0.9	0

Purified enzymes were incubated at 55°C and 60°C and subsequently their remaining activity was measured at 15°C. Representative time points are shown. Reported values are the average of at least two measurements. The standard deviations do not exceed 5%.

Previous studies (Lonhienne *et al*., 2000) suggested that the decreased values of the energy of activation, E_α, is the main characteristic property of psychrophilic enzymes with increased enzymatic activity at lower temperature. The E_α values for the wild-type and mutant enzymes were calculated from the slope of the Arrhenius plots in the temperature range 10–30°C (Fig. 3). All variants had higher E_α value than the native, cold-adapted TAB5 AP and thus lost the psychrophilic character of the reaction, except for the S86A variant (Table II). Variants S338T, H135E/G149D and S42G/S338T had almost four times greater E_α than the wild-type TAB5 AP (Table II).

We also calculated the specific contributions of entropy ($\Delta S^{\#}$) and enthalpy ($\Delta H^{\#}$) toward the overall free energy ($\Delta G^{\#}$) of activation for the wild-type TAB5 AP and its variants (Table II). Because k_{cat} is inversely proportional to $\Delta G^{\#}$

$$k_{cat} = \kappa(k_B T/h)e^{-\Delta G^{\#}/RT} \quad (4)$$

(Lonhienne *et al*., 2000), the $\Delta(\Delta G^{\#})_{wt\text{-}mut}$ parameter reflects the changes in k_{cat} between the compared enzymes. Positive $\Delta(\Delta G^{\#})_{wt\text{-}mut}$ values show that the psychrophilic wild-type enzyme is more active than most of the studied variants. H135E and H135E/G149D are the only ones which have a negative $\Delta(\Delta G^{\#})_{wt\text{-}mut}$ and consequently, they are more active than the native enzyme (Table II).

Differential scanning calorimetry

Wild-type TAB5 AP has a complex heat-induced unfolding pattern on DSC (Fig. 4, thick line). Structural changes are detected at a temperature as low as 35°C and are followed by a main unfolding transition centred around 45°C (Fig. 4). However, two discrete unfolding transitions also occur between 50°C and 65°C, before perturbation of the calorimetric signal by aggregation. This suggests that the enzyme conformation contains at least three structural regions differing by their intrinsic stability. As the wild-type AP unfolding is irreversible, and therefore kinetically driven, this also indicates that the unfolding pathway between the native and

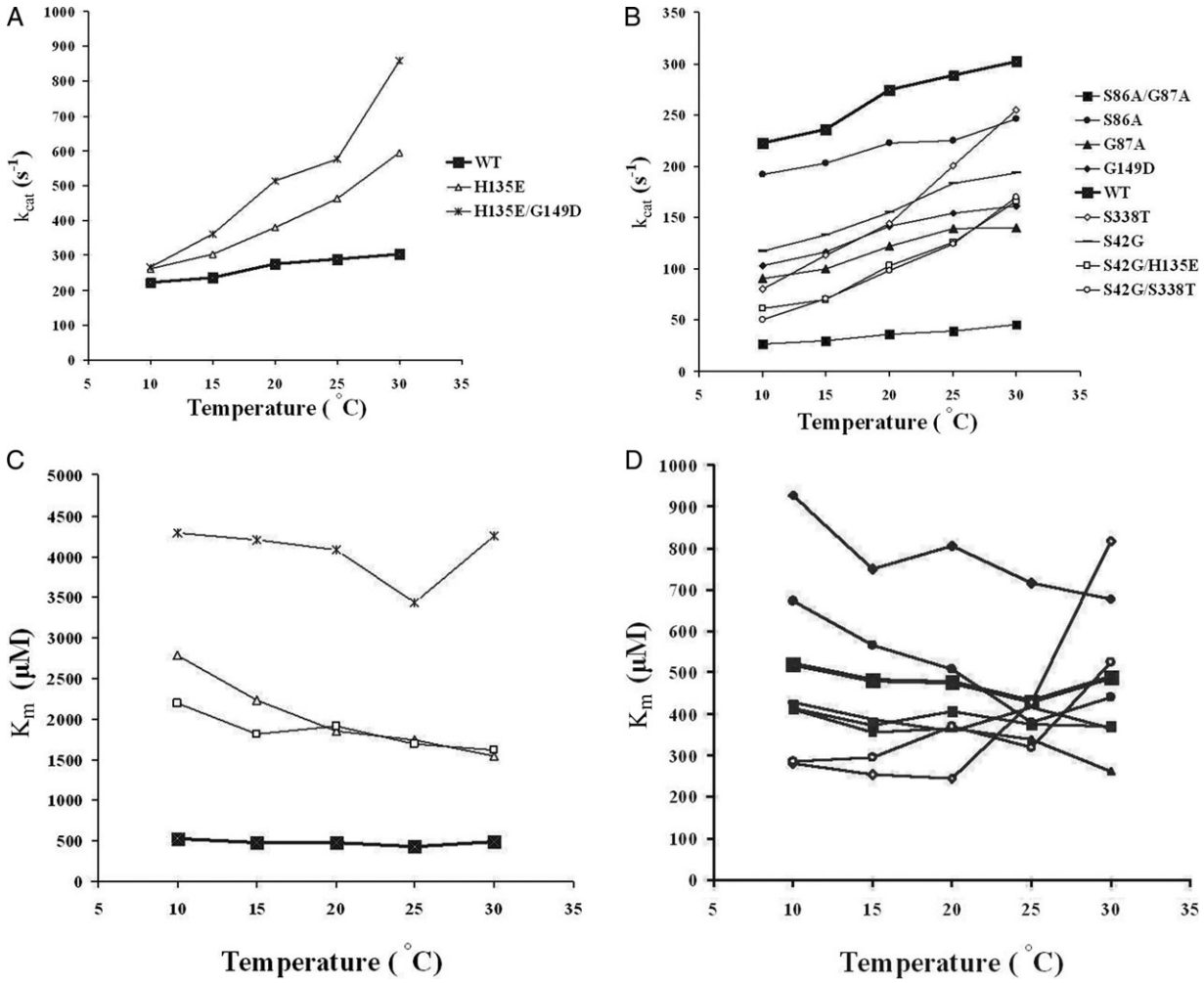

Fig. 2. Kinetic studies of wild-type and mutant APs. Temperature dependence of k_{cat} (**A** and **B**) and K_m (**C** and **D**) of wild-type and selected mutant APs at temperature range 10–30°C. All values were determined in a buffer containing 1 M diethanolamine-Cl pH 10, 10% glycerol, 10 mM $MgCl_2$, 1 mM $ZnCl_2$ and *p*NPP in various concentrations at 15°C. The k_{cat} values were calculated from V_{max} using a molecular weight for the enzyme of 35 861 Da. Reported values are the average of three measurements. The standard deviations do not exceed 5%. Symbols in C and D are as in A and B.

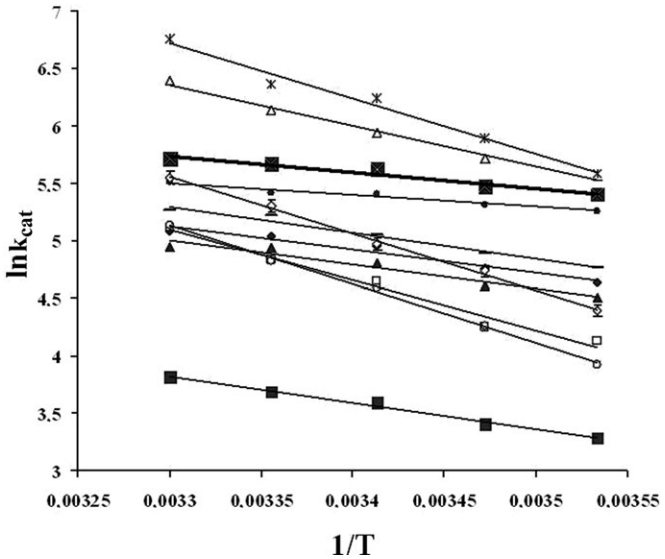

Fig. 3. Arrhenius plots for the k_{cat} of mutants and wild-type AP. Reported values are the average of three measurements. The standard deviations do not exceed 5%. Symbols are as in Fig. 2.

unfolded states passes through at least three intermediate states, differing by their kinetics of unfolding and resistance to heat denaturation. The thermograms of the mutant and wild-type APs are presented by increasing order of resistance against heat inactivation of the activity from the top to the bottom (Fig. 4). Each mutation and the combination of mutations produce a specific pattern of unfolding (Fig. 4). Interestingly, variants with increased residual activity (Table I) (lower curves, Fig. 4) are characterised in DSC by an increased T_m (top of the transition) of the first transition and the persistence of secondary transition(s) at higher temperatures. By contrast, mutants exhibiting decreased residual activity (Table I) (upper curves, Fig. 4) are characterised in DSC by the complete disappearance of unfolding intermediates around 60°C.

This behaviour is also correlated with the calorimetric enthalpy of the mutants (normalised area of the transition, corresponding to all enthalpy-driven interactions disrupted during unfolding). Indeed, there is no significant variation of ΔH_{cal} for mutants G149D, G87A and S86A that are resistant to heat inactivation (Table III). This can be explained by an

Table II. Enzymatic and thermodynamic parameters of the psychrophilic AP and of its mutants

Enzyme	k_{cat} (s^{-1})	E_α (kj/mol)	$\Delta G^{\#}$ (kj/mol)	$\Delta H^{\#}$ (kj/mol)	$T\Delta S^{\#}$ (kj/mol)	$\Delta(\Delta G^{\#})_{wt\text{-}mut}$ (kj/mol)	$\Delta(\Delta H^{\#})_{wt\text{-}mut}$ (kj/mol)	$T\Delta(\Delta S^{\#})_{wt\text{-}mut}$ (kj/mol)
WT	236	11.6	57.4	9.2	−48.2			
S86A	203	8.5	57.7	6.1	−51.6	0.3	−3.1	−3.4
G87A	100	17.2	59.4	14.8	−44.6	2	5.6	3.6
G149D	117	16.8	59	14.4	−44.6	1.6	5.2	3.6
S86A/G87A	30	19.1	62.3	16.7	−45.6	4.9	7.5	2.6
H135E/G149D	361	40.1	56.3	37.7	−18.6	−1.1	28.5	29.6
S42G	133	18.9	58.7	16.5	−42.2	1.3	7.3	6
H135E	303	29.4	56.8	27	−29.8	−0.6	17.8	18.4
S338T	114	40.9	59.1	38.5	−20.6	1.7	29.3	27.6
S42G/H135E	70	36.5	60.3	34.1	−26.2	2.9	24.9	22
S42G/S338T	71	42.6	60.2	40.2	−20	2.8	31	28.2

Reported values were determined at 15°C. E_α values were calculated from the slope of the Arrhenius plots in the temperature range 10–30°C (Fig. 3). Thermodynamic parameters $\Delta G^{\#}$, $\Delta H^{\#}$, $T\Delta S^{\#}$ were calculated as described in (Lonhienne *et al*., 2000).

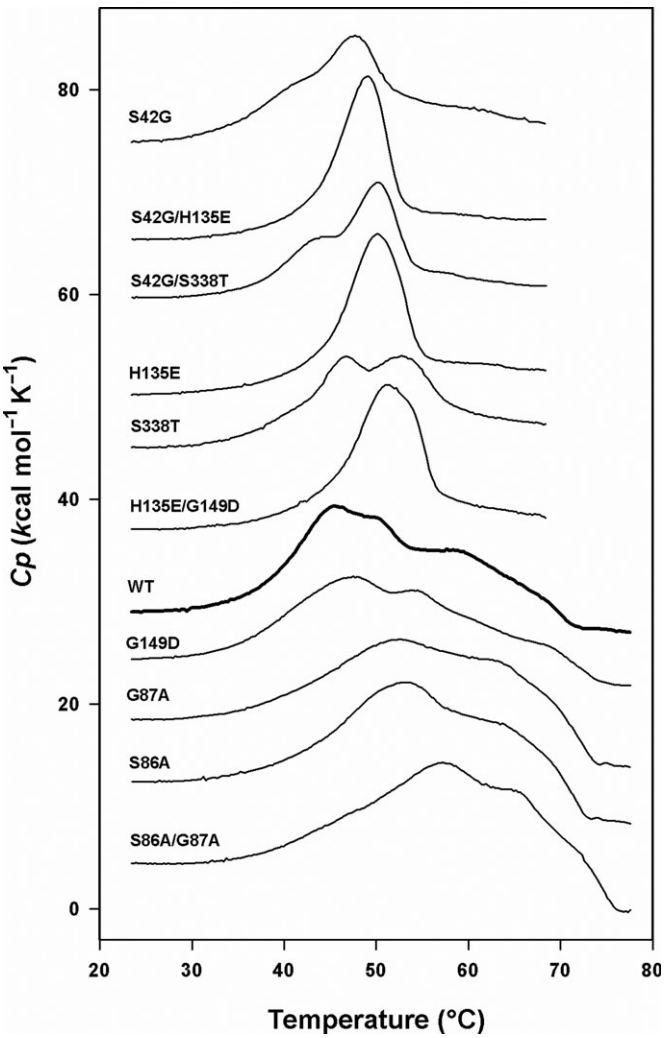

Fig. 4. Differential scanning calorimetry records of wild-type AP and of its mutants. Thermograms are normalised for protein concentration and have been displaced along the *y*-axis for clarity. Mutants displayed below wild-type AP are protected against heat inactivation of the activity and mutants displayed above wild-type AP have a reduced stability of the activity.

improved kinetic stability rather than enthalpic stabilisation. The latter only becomes significant for the double mutant S86A/G87A. In contrast, all mutants displaying reduced residual activity are also drastically destabilised as judged by the low ΔH_{cal} values. In this case, enthalpic destabilisation of the mutant structures seems to be the primary determinant of the weaker heat stability of the activity.

Table III. Microcalorimetric parameters of stability of wild-type AP and of its mutants

Enzyme	T_{m1} (°C)	T_{m2} (°C)	T_{m3} (°C)	ΔH_{cal} (kcal/mol)
S42G	41.7	47.7		78
S42G/H135E	49.0			91
S42G/S338T	44.8	50.3		72
H135E	50.2			98
S338T	46.5	52.7		97
H135E/G149D	51.2			109
WT	45.4	49.7	58.4	163
G149D	47.5	54.0		155
G87A	52.4	62.6		157
S86A	53.5	62.7		173
S86A/G87A	57.2	64.4		196

Discussion

Mutated residues in the three-dimensional structure of the TAB5 AP

We modelled the selected mutations to the TAB5 AP structure (Wang *et al*., 2007) (pdb code 2iuc) to understand the structural mechanism for the changes on the activity or stability of the enzyme. All selected mutations are located close to the active site, explaining their local effects on the enzyme activity (Fig. 5).

In the wild-type enzyme, S42 is preceding the Mg^{2+} (M3) and Zn^{2+} (M2) coordinating D43, which in the active site is on the opposite side of the catalytic S84 (Fig. 6B). S42 stabilises the end of a β strand by a side-chain interaction to S300 on the neighbouring strand and thus affirms stable position for the metal coordinating D43 and D301 (Fig. 6B). Mutation S42G removes this interaction and affects the stability of Mg^{2+} and Zn^{2+} (M2) coordination resulting in a less stable enzyme (Table III) with reduced hydrolytic activity (Fig. 2B).

The active site nucleophile at S84 is preceded by an α-helix containing both residues S86 and G87 (Fig. 6A). The effects of these mutations are probably best explained

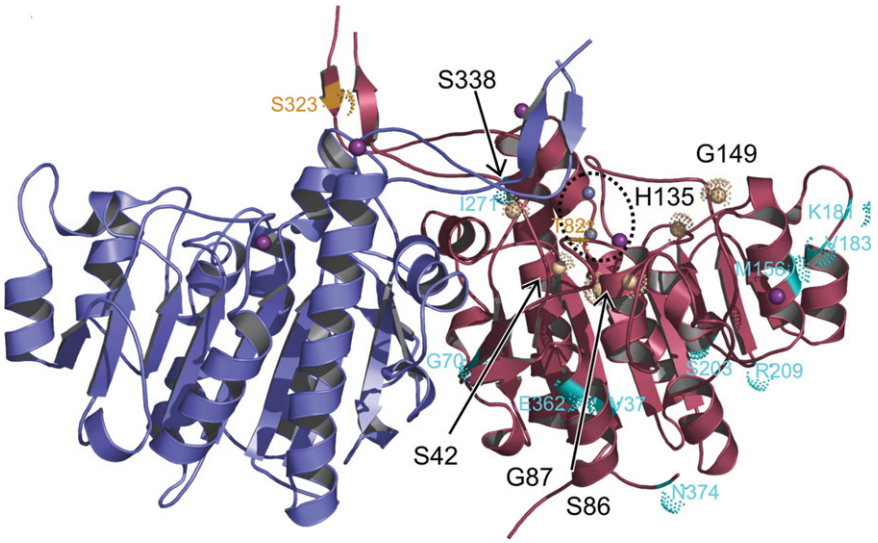

Fig. 5. The overall structure of the homodimeric wild-type TAB5 AP (Wang *et al*., 2007) (pdb, 2iuc). The monomers of the TAB5 AP dimer are coloured in red and blue. The active site containing the metal ions is circled by a dotted line and selected mutated sites are indicated by brown balls. All characterised mutations were located close to the active site. Mutations that were not further characterised are in cyan (increased residual activity) and yellow (decreased residual activity).

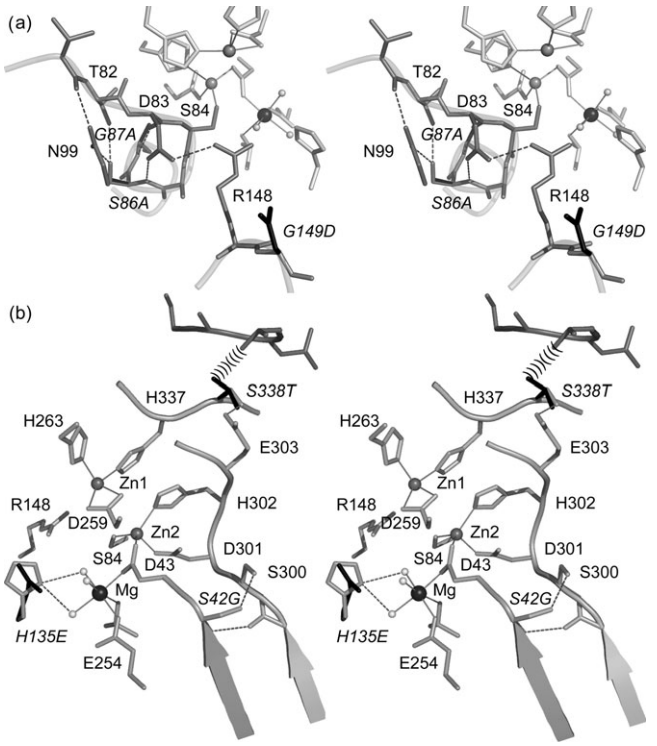

Fig. 6. A detailed stereo-image showing the characterised mutations in the TAB5 AP structure (pdb, 2iuc,Wang *et al*., 2007) (**A**) displaying mutations S86A, G87A and G149D and (**B**) H135E, S42G and S338T. Native structure is in grey and mutated residues in black, Zn^{2+} and Mg^{2+} are in dark grey and black, respectively. Metal coordination is shown with solid and hydrogen bonds with dotted lines.

through accurate positioning of S84, which is covalently modified during the first step of catalysis (Stec *et al*., 2000). The side chain of S86 is holding together the S84 containing loop by interactions with T82 and N99. In addition in the α-helix, the backbone G87(N) ends the turn from D83(O) thus possibly affecting the flexibility of another central residue in the active site, as the side chain of D83 is stabilising R148 which is thought to interact with the product phosphate (Fig. 6A). The two alanine mutations remove the side-chain interactions from S86 and affect the flexibility of G87.

H135 is involved in Mg^{2+} binding in the active site of TAB5AP (Fig. 6B). Although H135 does not directly coordinate the Mg^{2+} metal ion in the TAB5 AP structure, it has been suggested to affect the metal specificity at the third metal position (Wojciechowski and Kantrowitz, 2002). Mutation H135E causes distortion of the metal binding site and weaker binding of Mg^{2+} resulting to a destabilised enzyme with increased k_{cat} (Fig. 2A). In destabilised enzyme variant S42G/H135E k_{cat} is drastically reduced when compared with the other two mutants bearing the H135E mutation (Fig. 2A and B) reflecting the important role of stabilisation of the active site by metal ions in catalysis.

G149 affects the flexibility of R148 and could affect the stability of phosphate/substrate coordination during catalysis (Fig. 6A). Mutation G149D restricts the movements of the R148 loop, so that residue R148 cannot adapt to the conformational changes of the active site during catalysis resulting in a less active enzyme (Fig. 2B). The reduced flexibility of the backbone due to the mutation G149D also explains the reduced unfolding enthalpy for this mutation (Table III).

In double mutant H135E/G149D, the effect of mutation G149D on R148 is reversed; the active site adjusts again to the formation of the reaction intermediates. This structural effect could result in the increased activity of H135E/G149D when compared with the H135E variant (Fig. 2A). H135 is also in 4 Å distance from the head of the substrate coordinating residue R148. When the charge of this residue (in H135E) changes, it could affect the entropy of substrate coordination, in the ground state as well as during catalysis. This effect would probably also be monitored by Mg^{2+} binding; when the metal ion is bound, 135E prefers metal coordination and does not effect R148 flexibility. However, as the metal binding is weaker, in the absence of metal ion

135E could restrict free adjustments on R148 conformation as well as interfere with the binding of the negatively charged phosphoryl groups.

S338 is on the interface of the two monomers and the side-chain hydrogen bonds to E303 (Fig. 6B). Mutation S338T can probably also make this interaction by directing the branched side chain to a fairly tightly packed interface region, but this may destabilise the position of the M1 metal coordinating H337 affecting the stability of the enzyme (Table III). The S42G/S338T variant combines two destabilising mutations and results in a variant, which has the lowest ΔH_{cal} (Table III).

Remarkably, three out of six of the selected mutations involve a change in a glycine residue (mutations S42G, G87A and G149D). The importance of a glycine cluster in the cold adaptation of the enzyme was also noted in a previous mutagenesis study on TAB5 AP (Mavromatis *et al*., 2002). These data highlight the unique properties of this amino acid in contributing to the psychrophilic characteristics of the enzyme.

However, there were amino acid substitutions obtained outside the catalytic cavity, scattered in several regions of the enzyme (Fig. 5). Mutations V37I, G70C, M156R, K181E, V183G, S203P, R209S, I271N, E362G and N374K resulted in slightly stabilised enzymes, while mutants S323R and T82S exhibited subtle destabilising effects. Nonetheless, their further characterisation or usage as templates for *in vitro* DNA recombination experiments was not attempted since they all exhibited initial and residual activity (after thermal treatment) values differing less than 10% compared to the wild type (data not shown).

Activity at low temperatures

An increase of k_{cat} may be achieved enthalpically through a decrease in $\Delta H^{\#}$ or entropically through an increase in $\Delta S^{\#}$

$$k_{cat} = \kappa(k_B T/h)e^{-(\Delta H^{\#}/RT - \Delta S^{\#}/R)} \quad (5)$$

The S86A variant has an increased T_m profile and it thus appears stabilised. However, it is the only variant which retains and even enhances the psychrophilic character of the enzyme (decreased $\Delta H^{\#}$ and E_α). However, due to $\Delta S^{\#}$ decrease, it does not appear more active than the wild-type AP (Table II, Fig. 2B). The rest of the mutants have lost their psychrophilic character since they have increased $\Delta H^{\#}$ and E_α values (Table II).

The negative entropy values for the wild-type and AP variants suggest that the activated transition state of catalysis is more ordered than the ground state (Table II). Mutants H135E and H135E/G149D despite having increased $\Delta H^{\#}$ values are more active than the wild type due to an increase of the $\Delta S^{\#}$. Higher $\Delta S^{\#}$ is achieved by reducing the distribution of the conformational states of the enzyme-substrate complex and decreasing of the negative effect of $\Delta(\Delta S^{\#})$ that acts on k_{cat} (Lonhienne *et al*., 2000).

Concluding remarks

Studies employing rational and non-rational design have provided significant information towards understanding the mechanisms of cold adaptation. In the current study, TAB5 AP was subjected into *in vitro* evolution pressure in order to identify specific residues important for psychrophilic AP activity and stability.

All most drastic effects on these evaluated properties were due to changes around the active site. This is not a result of the screening method since we also found mutations outside the catalytic cavity. However, they were not selected for further characterisation due to the small effects they exerted on the measured enzyme properties. Based on our random mutagenesis study, we thus conclude that the active site of this psychrophilic protein is of great importance for both enzyme activity and stability.

Even single-point mutations in the active site can drastically change the unfolding pathway of the enzyme as also observed for phosphoglucose isomerase and inorganic pyrophosphatase (Halonen *et al*., 2005; Hansen *et al*., 2005). All the engineered AP variants exhibited a complete disappearance of unfolding transitions and large shifts of the T_m values. Furthermore, stabilised mutants unfold over a broad range of temperatures, resulting in a shallow transition and a low cooperativity of unfolding whereas destabilised mutants display sharper transitions suggesting higher unfolding cooperativity. This finding is consistent with adjustments of the kinetic stability. Stable enzymes slow down the unfolding rate by introducing unfolding intermediates and low unfolding cooperativity, whereas unstable proteins are characterised by a more uniformly heat-labile structure that increase the unfolding rate (D'Amico *et al*., 2003).

The stabilised variants S86A, G87A, S86A/G87A and G149D had lower k_{cat} and K_m values (Fig. 2B and D) while the two destabilised variants H135E/G149D and H135E that have an improved activity also display much higher K_m values (Fig. 2A and C). This is in agreement with the observation that a higher activity is gained at the expense of substrate affinity in cold-active and heat-labile enzymes (Feller, 2003). S42G, S338T, S42G/S338T and S42G/H135E, however, demonstrate that destabilisation is not sufficient to improve k_{cat} (Fig. 2B). Several structural constraints need to be satisfied also to maintain cold-adapted enzyme activity.

Comparison of H135E/G149D and H135E mutants reveals that insertion of the stabilising mutation G149D to the H135E variant results in a simultaneous increase of stability (Table III) and activity (Fig. 2A). These variants demonstrate that the activity–stability relationship can be modified by slight changes in the protein structure. This demonstrates that low temperature activity and thermostability can be improved simultaneously, though this rarely happens through natural selection. The observation is in agreement with previous studies (Van den Burg *et al*., 1998; Miyazaki *et al*., 2000). Directed evolution is thus a powerful approach for the discovery of the physical and chemical limitations of a protein structure free of nature's biological and environmental constraints. Different combinations of mutations can change the relationship of the enzyme properties in any direction, highlighting the delicate balance that exists among stability and activity.

Funding

General Secretariat for Research and Technology of Greece (PENED 2001, 01εΔ311); National Norwegian Program in Functional Genomics (FUGE).

References

Arnold,F.H. (2001) *Nature*, **409**, 253–257.

Arnold,F.H. and Moore,J.C. (1997) *Adv. Biochem. Eng. Biotechnol.*, **58**, 1–14.

Bradford,M.M. (1976) *Anal. Biochem.*, **72**, 248–254.

Cadwell,R.C. and Joyce,G.F. (1994) *PCR Methods Appl.*, **3**, S136–S140.

Cavicchioli,R., Siddiqui,K.S., Andrews,D. and Sowers,K.R. (2002) *Curr. Opin. Biotechnol.*, **13**, 253–261.

Coleman,J.E. and Gettins,P. (1983) InSpiro,T.G.(ed.), *Metal Ions in Biology*, vol. 5. John Wiley and Sons, New York, pp. 153–217.

Dalby,P.A. (2003) *Curr. Opin. Struct. Biol.*, **13**, 500–505.

D'Amico,S., Gerday,C. and Feller,G. (2001) *J. Biol. Chem.*, **276**, 25791–25796.

D'Amico,S., Claverie,P., Collins,T., Georlette,D., Gratia,E., Hoyoux,A., Meuwis,M.A., Feller,G. and Gerday,C. (2002) *Philos. Trans. R. Soc. Lond. B Biol. Sci.*, **357**, 917–925.

D'Amico,S., Marx,J.C., Gerday,C. and Feller,G. (2003) *J. Biol. Chem.*, **278**, 7891–7896.

Emsley,P. and Cowtan,K. (2004) *Acta Crystallogr. D Biol.Crystallogr.*, **60**, 2126–2132.

Feller,G. (2003) *Cell. Mol. Life Sci.*, **60**, 648–662.

Fields,P.A. and Somero,G.N. (1998) *Proc. Natl Acad. Sci. USA*, **95**, 11476–11481.

Gerday,C., *et al*. (2000) *Trends Biotechnol.*, **18**, 103–107.

Gianese,G., Bossa,F. and Pascarella,S. (2002) *Proteins*, **47**, 236–249.

Giver,L., Gershenson,A., Freskgard,P.O. and Arnold,F.H. (1998) *Proc. Natl Acad. Sci. USA*, **95**, 12809–12813.

Halonen,P., Tammenkoski,M., Niiranen,L., Huopalahti,S., Parfenyev,A.N., Goldman,A., Baykov,A. and Lahti,R. (2005) *Biochemistry*, **44**, 4004–4010.

Hansen,T., Schlichting,B., Grotzinger,J., Swan,M.K., Davies,C. and Schonheit,P. (2005) *FEBS J.*, **272**, 6266–6275.

Horton,R.M., Cai,Z.L., Ho,S.N. and Pease,L.R. (1990) *Biotechniques*, **8**, 528–535.

Jaenicke,H., Schurig,H., Beaucamp,N. and Ostendorp,R. (1996) *Adv. Protein Chem.*, **48**, 181–269.

Laemmli,U.K. (1970) *Nature*, **227**, 680–685.

Lin,H. and Cornish,V.W. (2002) *Angew. Chem. Int. Ed. Engl.*, **41**, 4402–4425.

Lonhienne,T., Gerday,C. and Feller,G. (2000) *Biochim. Biophys. Acta*, **1543**, 1–10.

Margesin,R., Feller,G., Gerday,C. and Russell,N.J.. (2002) In Bitton,G.(ed.), *Encyclopedia of Environmental Microbiology*, **vol. 2**. John Wiley and Sons, New York, pp. 871–885.

Martin,A., Sieber,V. and Schmid,F.X. (2001) *J. Mol. Biol.*, **309**, 717–726.

Mavromatis,K., Tsigos,I., Tzanodaskalaki,M., Kokkinidis,M. and Bouriotis,V. (2002) *Eur. J. Biochem.*, **269**, 2330–2335.

Mavromatis,K., Feller,G., Kokkinidis,M. and Bouriotis,V. (2003) *Protein Eng.*, **16**, 497–503.

Miyazaki,K., Wintrode,P.L., Grayling,R.A., Rubingh,D.N. and Arnold,F.H. (2000) *J. Mol. Biol.*, **297**, 1015–1026.

Richards,F.M. (1997) *Cell. Mol. Life Sci.*, **53**, 790–802.

Rina,M., Pozidis,C., Mavromatis,K., Tzanodaskalaki,M., Kokkinidis,M. and Bouriotis,V. (2000) *Eur. J. Biochem.*, **267**, 1230–1238.

Smalas,A.O., Leiros,H.K., Os,V. and Willassen,N.P. (2000) *Biotechnol. Annu. Rev.*, **6**, 1–57.

Spiller,B., Gershenson,A., Arnold,F.H. and Stevens,R.C. (1999) *Proc. Natl Acad. Sci. USA*, **96**, 12305–12310.

Stec,B., Holtz,K.M. and Kantrowitz,E.R. (2000) *J. Mol. Biol.*, **299**, 1303–1311.

Tsigos,I., Mavromatis,K., Tzanodaskalaki,M., Pozidis,C., Kokkinidis,M. and Bouriotis,V. (2001) *Eur. J. Biochem.*, **268**, 5074–5080.

Van den Burg,B., Vriend,G., Veltman,O.R., Venema,G. and Eijsink,V.G. (1998) *Proc. Natl Acad. Sci. USA*, **95**, 2056–2060.

Wang,E., Koutsioulis,D., Leiros,H.S., Andersen,O.E., Bouriotis,V., Hough,E. and Heikinheimo,P. (2007) *J. Mol. Biol.*, **366**, 1318–1331.

Wintrode,P.L. and Arnold,F.H. (2000) *Adv. Protein Chem.*, **55**, 161–225.

Wintrode,P.L., Miyazaki,K. and Arnold,F.H. (2001) *Biochim. Biophys. Acta*, **1549**, 1–8.

Wojciechowski,C.L. and Kantrowitz,E.R. (2002) *J. Biol. Chem.*, **277**, 50476–50481.

Yano,J.K. and Poulos,T.L. (2003) *Curr. Opin. Biotechnol.*, **14**, 360–365.

Zavodszky,P., Kardos,J., Svingor,A. and Petsko,G.A. (1998) *Proc. Natl Acad. Sci. USA*, **9**, 7406–7411.

Zhao,H. and Arnold,F.H. (1997) *Curr. Opin. Struct. Biol.*, **7**, 480–485.

Zhao,H., Giver,L., Shao,Z., Affholter,J.A. and Arnold,F.H. (1998) *Nat. Biotechnol.*, **16**, 258–261.

Received November 15, 2007; revised February 10, 2008; accepted February 20, 2008

Edited by Frances Arnold